ACS APPLIED MATERIALS & INTERFACES

RESEARCH ARTICLE

www.acsami.org

Understanding the Effect of Surface Chemistry on Charge Generation and Transport in Poly (3-hexylthiophene)/CdSe Hybrid Solar Cells

Jun Yan Lek,[†] Lifei Xi,[†] Beata E. Kardynal,[‡] Lydia Helena Wong,[†] and Yeng Ming Lam*[,†]

[†]School of Materials Science and Engineering, Nanyang Technological University, 50 Nanyang Avenue, Singapore 639798 and

[‡]Department of Photonics Engineering, Technical University of Denmark, DTU Fotonik, Ørsteds Plads 343, 2800 Kgs. Lyngby, Denmark

Supporting Information

ABSTRACT: For hybrid solar cells, interfacial chemistry is one of the most critical factors for good device performance. We have demonstrated that the size of the surface ligands and the dispersion of nanoparticles in the solvent and in the polymer are important criteria in obtaining optimized device performance. The size of the ligands will affect the charge transport at the particle/particle and particle/polymer interfaces and the chemical structures of the ligands will determine their compatibility with the solvent and polymer. Hence other than pyridine, 2-thiophenemethylamine also showed good potential as ligand replacement for poly-(3-hexylthiophene)/CdSe hybrid solar cells. With the right ligand combination, we have shown that the power conversion efficiency improved by a factor of 6 after ligand exchange.

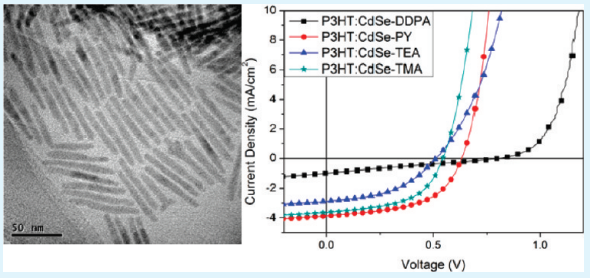

KEYWORDS: hybrid photovoltaics, ligand exchange, surface chemistry, dispersion, conductivity

INTRODUCTION

Stringent fabrication requirements and the high production cost of silicon-based inorganic photovoltaics have greatly limited the reduction in the cost of solar cells. Therefore, organic and organic−inorganic hybrid photovoltaics that offer solution-processable, low-cost, and large-area fabrication play an important role in realizing low-cost solar cells. Organic solar cells which consist of poly (3-hexylthiophene) (P3HT) and fullerene derivatives have achieved power conversion efficiencies (PCE) as high as 5%.[1,2] The solar absorption in organic solar cells is limited by the relatively wide band gap of the organic molecules, which do not usually absorb in the infrared region. This can be circumvented by using inorganic semiconducting nanoparticles, such as cadmium selenide (CdSe),[3−6] or lead sulfide (PbS), with tunable band gaps and higher electron mobilities as electron acceptor candidates blended with semiconducting polymers in bulk heterojunction hybrid solar cells.[7]

Generally, surfactants or ligands are present during the synthesis of inorganic nanoparticles. They serve as a stabilizing agent to prevent aggregation, mediate the growth and also passivate the surface states.[8] However, these long alkyl chain ligands, such as trioctylphosphine oxide (TOPO), phosphonic acids, oleic acids, etc., often act as an insulating barrier that hinder the charge transfer between electron donors and nanocrystals, and the charge transport between the inorganic nanoparticles when they are incorporated into hybrid photovoltaics. Various molecules have been used as new ligands to replace the original long insulating ligands. Short ligands, such as pyridine and butylamine, are able to reduce the interparticle spacing and hence give rise to more efficient charge transfer; however, this may be at the expense of the solubility of these nanocrystals in common organic solvents and the dispersibilty in polymers and hence, binary solvent was used to improve their dispersion in the blend films. As a result, both ligands have been shown to improve the device performances.[3,9] Besides these, other small organic molecules such as thiols and amines have also been employed as new ligands.[9−11] Another strategy in the selection of suitable surface ligands is to select molecules with similar moieties to the polymer in order to enhance the compatibility of the nanocrystals with the polymer, such as oligothiophene moieties;[12] however, little data have been reported so far. From the above discussion, one can see that there are some important considerations for the replacement ligands. Two such considerations are how insulating are the ligands to charge transport and their effect on dispersion of the nanoparticles first in the solvent and then in the polymer. To date, discussions of these hybrid systems seem to imply that a single "ideal" ligand will improve the device performance but due to the multitude of considerations ranging from controlling the synthesis to charge transport to dispersion, a combination of ligands may be a better solution for such blend systems.

Received: September 30, 2010
Accepted: January 2, 2011
Published: January 24, 2011

In this letter, we report the photovoltaic performance of hybrid photovoltaic devices comprised of ligand-exchanged CdSe nanorods blended with P3HT. Different ligands were exchanged for dodecylphosphonic acid (DDPA) capped on the CdSe nanorods. The selection of the ligands were based on: (a) size, small molecules are used; (b) compatibility between the end groups of ligands and solvent/polymer; and (c) affinity of the headgroup to CdSe.[12] With these considerations in mind, we selected 2-thiophenemethylamine (TMA) and 2-thiopheneethylamine (TEA) to compare with the commonly used pyridine (PY). We will show that a combination of ligands that effectively improves the different aspects of the system gives the most optimized behavior.

EXPERIMENTAL SECTION

As shown in Figure 1a, CdSe nanorods with a diameter of around 7 nm and length 70 nm ±10 nm were synthesized using the hot coordinating solvents method.[13] In a typical CdSe nanoparticle synthesis, 256 mg (2 mmol) of cadmium oxide (CdO), 1.0 g (4 mmol) of DDPA, and 2.5 g of TOPO were loaded into a three-necked flask equipped with a condenser and thermometer. The mixture was then heated up to 330 °C. At elevated temperature, the solution mixture turned colorless indicating the formation of Cd-DDPA complexes. The solution was cooled to 310 °C and held at constant temperature. A selenium precursor solution containing 156 mg (2 mmol) of Se powder and 2.0 g of trioctylphosphine (TOP) was injected into the Cd precursor solution in multiple injections (4 times at 2 min intervals). The nanocrystals were allowed to grow for 30 min. The reaction was stopped by removal of the reaction flask from the heating mantle. The CdSe nanorods were washed several times with anhydrous toluene and anhydrous methanol.

Ligand exchange was carried out to remove the original ligands that were used in the synthesis and replaced them with new ligands. Pyridine, TMA, and TEA were used as new ligands in this study (Figure 1a). The ligand exchange method for pyridine is adopted and modified from ref 14. CdSe nanorods were stirred in an excess of pyridine under nitrogen reflux at 60 °C for 4 days. The nanocrystals were precipitated with excess n-hexane and redispersed in pyridine. For ligand exchange using TEA and TMA, CdSe nanorods were stirred in an excess of ligands in chloroform under nitrogen reflux at 45 °C for 4 days. The ligand exchanged CdSe nanocrystals were dispersed in chloroform and precipitated using excess acetone. All CdSe nanoparticles were dried in a vacuum overnight to remove excess solvent.

For the fabrication of P3HT:CdSe hybrid photovoltaics, ligand-capped CdSe nanorods were dispersed in 1,2-dichlorobenzene (DCB) or chloroform. CdSe solutions and P3HT solutions were mixed together to form a blend solution containing 90 wt % CdSe in polymer. A layer of PEDOT:PSS was spin-coated on plasma-cleaned indium tin oxide (ITO) coated glass substrates and baked at 140 °C for 10 min. Next, about 80−100 nm of active layer was then spin-coated on the substrate under a nitrogen environment. An aluminum cathode was deposited by thermal evaporation to form a device area of 0.07 cm^2. The devices were then annealed at 150 °C for 30 min. For devices made of pyridine-capped CdSe nanoparticles, the fabrication was similar but 10 vol % pyridine was used together with DCB or chloroform to help in the dispersion of the nanorods in solution.[3]

The morphology of CdSe nanorods were determined using a JEOL 2010 transmission electron microscope (TEM) fitted with a LaB_6 filament operating at an acceleration voltage of 200 kV. The amount of organic ligands on the nanoparticles was determined using a TA Instruments (TGA2950) thermogravimetric analyzer. The thickness of the blend films were measured using a KLA Tencor Alpha- StepIQ surface profilometer. The current density−voltage ($J-V$) characteristics of the devices were measured using a Keithley 2400 SMU in ambient at 1 sun (AM1.5G, 100 mW/cm^2) illumination simulated by a Newport model 66902 solar simulator. Atomic force microscope (AFM) images were obtained using a Digital Instrument Nanoscope IIIa.

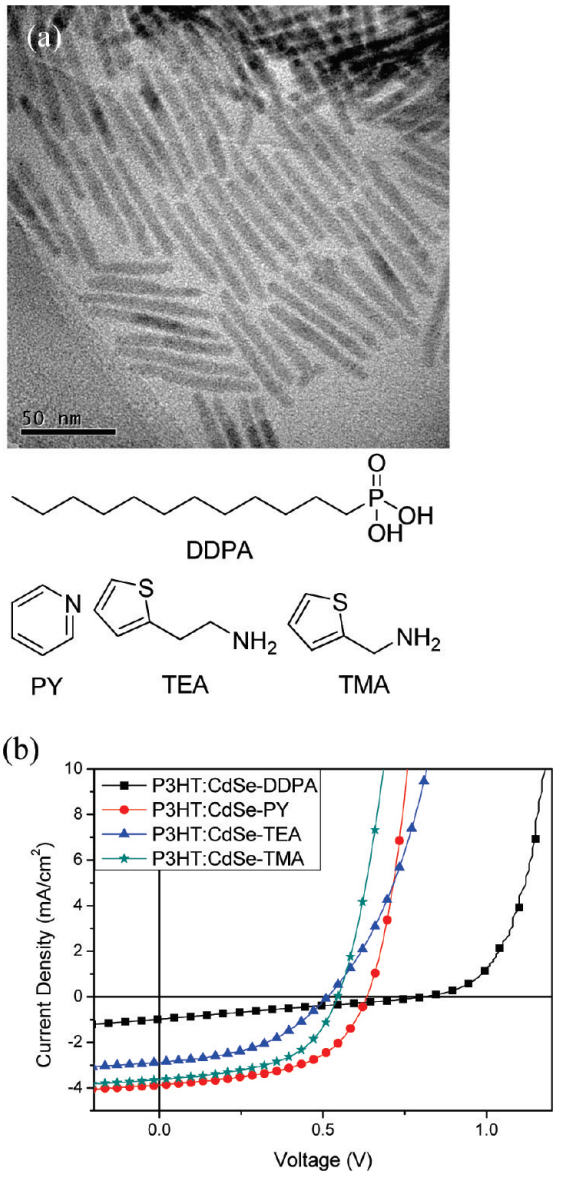

Figure 1. (a) TEM image of CdSe nanorods and the chemical structure of the ligands used in this study. (b) Current density−voltage characteristic of P3HT:CdSe (different capping ligands) hybrid photovoltaic devices under 1 sun illumination. DCB is used as the solvent.

RESULTS AND DISCUSSION

Figure 1b shows the $J-V$ characteristic of four different P3HT:CdSe hybrid devices made with CdSe nanorods with different capping ligands under 1 sun illumination. The photovoltaic properties are summarized in Table 1. The performance of all the devices improved after ligand exchange. It can be accredited to the removal of some of the original insulating ligands resulting in an enhanced charge transport. Among the three ligands used in this study, devices made from pyridine-capped CdSe nanorods performed better than the other two ligands and its PCE improved by six times as compared to that

before ligand exchange. CdSe-TMA devices performed very similarly to CdSe-PY devices except for the V_{OC} (0.1 V difference). This can be attributed to the perturbation of the energy levels of CdSe nanorods caused by the different surface modification. The LUMO of the TMA-capped CdSe nanorods (−3.9 eV) is lower than the LUMO of PY-capped CdSe nanorods (−3.8 eV), calculated from the cyclic-voltammogram (data not shown). Although the chemical structures of TEA and TMA are similar, the PCE value for CdSe-TEA device was only 63% of the CdSe-TMA devices due to the lower J_{SC} and FF values. In this study, we also investigated the performances of the devices made from chloroform. It is found that they follow a similar trend to those made using DCB as the solvent as shown in Table S1 in the Supporting Information. The differences in performance of the devices with different surface chemistries may be due to the degree of ligand exchange, the dispersibility of the nanocrystals in the solvent (after the exchange) and the polymer, or the conductivity of the ligands. Next, we will look at which of the above factors is likely to cause the observed device performance.

Thermogravimetric analysis (TGA) was used to characterize the ligand coverage on the CdSe nanorod surface and the results are shown in Figure 2. As the non-ligand-exchanged CdSe nanoparticles were heated, two steps of weight loss can be observed. The more prominent one occurs at about 430 °C and can be assigned to the decomposition of DDPA on the nanocrystals. Although some fraction of the ligands could be TOPO and triocylphosphine (TOP), it is most probable that phosphonic acids instead of TOPO were bound on the nanocrystals surface. Using H^1 NMR, Z. A. Peng et al. observed that in a similar synthetic system, the ligands on the CdSe nanoparticle surface were mainly phosphonic acids.[15] The smaller drop that appears at 250 °C is probably caused by the loss of other phosphonic species, which are loosely attached on the surfaces.[16]

Table 1. Summary of P3HT:CdSe Hybrid Device Performance with Different Surface Ligands and Solvents; PCE Refers to Power Conversion Efficiency, J_{SC} Refers to Short-Circuit Current Density, V_{OC} Refers to Open-Circuit Voltage and FF Refers to Fill Factor

ligand	solvent	PCE (%)	J_{SC} (mA/cm^2)	V_{OC} (V)	FF
DDPA	DCB	0.20	0.98	0.81	0.25
PY	DCB+PY	1.31	3.87	0.64	0.53
TEA	DCB	0.66	2.89	0.51	0.45
TMA	DCB	1.05	3.64	0.55	0.53

The weight loss due to the DDPA portion before and after ligand exchange can be determined from the TGA data (Figure 2). About 27, 77, and 64% of DDPA was removed from CdSe-PY (Figure 2a), CdSe-TEA (Figure 2b) and CdSe-TMA (Figure 2c) nanorods, respectively. From the weight loss measured by TGA we can estimate the surface ligand coverage for CdSe nanorods before and after ligand exchange, bearing in mind the following assumptions: weight losses in the TGA plots are solely contributed by the lost of organic substances on the nanorods and the organic ligands bind only on Cd atoms.[16] Assuming the CdSe nanorods is uniform and cylindrical, the ligand packing factor for the nanorods can be calculated. For each nanorod, the fraction of surface Cd sites that are covered by organic ligands, γ, is given by $\gamma = (X_{org}M_{core})/(SM_{org}(1-X_{org}))$, where M_{core} is the mass of CdSe, X_{org} is the mass fraction of organic species given from TGA analysis, M_{org} is the mass of one organic ligand, and S denotes the amount of Cd sites on the surface of nanocrystals. Both S and M_{core} are given by: $M_{core} = \pi r^2 lm$ and $S = (\{\pi r^2 l - [\pi(r-d)^2(l-2d)]\}N)/(V)$. In these expressions, r and l refer to the radius and length of the nanorods, respectively, and m refers to the specific mass of CdSe. V denotes the volume of a CdSe unit cell, N is the number of CdSe in a unit cell and d is the Cd − Se bond length. Kuno et al. and Foos et al. used a similar model to calculate the surface ligand packing factor for spherical CdSe nanoparticles.[16,17] Using this model, the surface coverage of DDPA, γ_{DDPA}, is found to range from 0.47 to 0.57 before ligand exchange. The γ value indicates that about 50% of the Cd atoms at the surface are covered with DDPA, which suggests a relatively packed ligand shell surrounding the nanocrystals considering the bulky structure of DDPA.

After ligand exchange, it is obvious that there is a two-step mass loss in the TGA plots: the one at lower temperature is attributed to decomposition of the replacing ligands, and the one at higher temperature comes from the original DDPA. Surface coverage of the replacing and original ligands can be calculated based on the earlier discussion. In CdSe-PY case, γ_{DDPA} was reduced to 0.41, whereas γ_{PY} is 0.33. γ_{DDPA} of CdSe-TEA and CdSe-TMA are 0.10 and 0.17 after ligand exchange. γ_{TEA} and γ_{TMA} are 0.68 and 0.62, correspondingly. It was observed that after ligand exchange more than 70% of the surface of the nanocrystals are covered by organic ligands. In all cases, it was found that on average every DDPA molecule was replaced by two replacing ligands. This suggested that during ligand exchange, two new ligands can be accommodated into the empty sites for every DDPA molecule removed from the surface of the nanorods due to their smaller size compared to DDPA and eventually increase the packing density of ligands. The densely packed

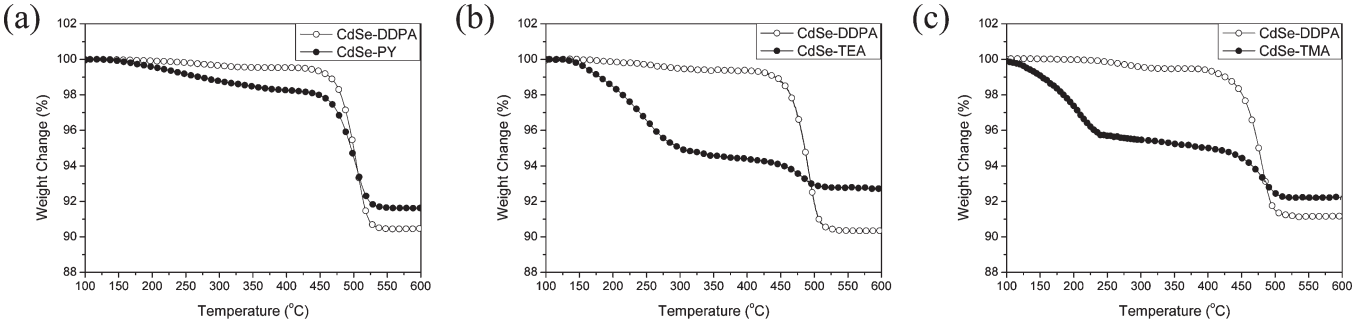

Figure 2. Thermogravimetric analysis (TGA) plot of weight change as a function of the temperature of CdSe nanorods before (open circles) and after (solid circles) ligand exchange for: (a) PY, (b) TEA and (c) TMA.

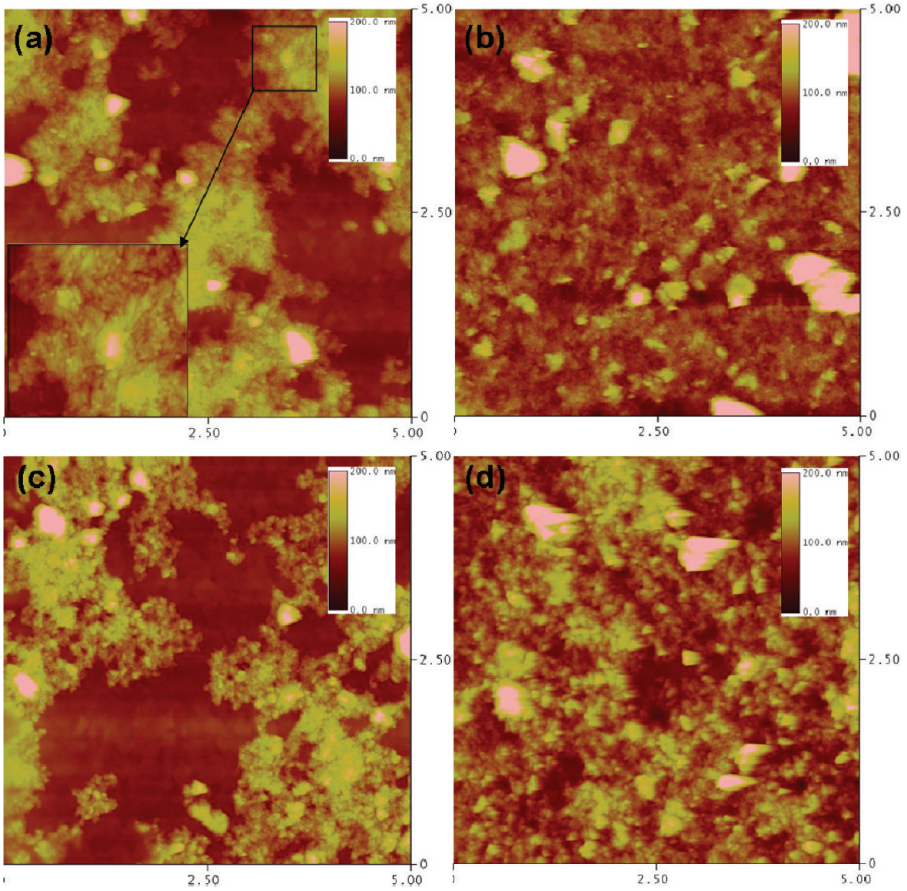

Figure 3. Tapping mode AFM images of the P3HT:CdSe blend film with different surface ligands (a) DDPA, (b) PY, (c) TEA, and (d) TMA casted from DCB. (for CdSe-PY, 10% of pyridine was added as a host solvent). The scan size is 5 μm × 5 μm. Inset in image a shows clearly the nanorods at higher magnification.

ligand layer implies that the charge transfer between the nanoparticles and the polymer has to flow through the ligand shell. This is probably one of the important current controlling factors.

Although TEA and TMA devices have a similar replacement efficiency, J_{SC} of the TMA device is higher by more than 25% (Table 1). The replacement efficiency may not be the dominant factor for this variation. J_{SC} variation can also be due to the connectivity of the pathways for the charge transportation to the respective electrodes. Hence next we will look at the blend morphology using an AFM operating in tapping mode.

DDPA is commonly used in synthesis not only to mediate nanocrystal growth, but also to provide reasonably good solubility for nanocrystals in common organic solvents.[18] CdSe-DDPA dispersed very well in DCB and chloroform, whereas CdSe-PY, CdSe-TEA and CdSe-TMA dispersed well in the polymer. Therefore the morphology of the hybrid films can be influenced by the extent of ligand exchange due to this difference in the solubility of the nanorods in the solvent and polymer. Figure 3 shows tapping mode AFM images of the four P3HT:CdSe hybrid devices. Looking at Figure 3a, the P3HT:CdSe-DDPA hybrid film appears to be phase separated. This is likely to be due to the incompatibility between DDPA and P3HT in the blend. The brighter regions in the film are CdSe nanorod aggregates. The nanorods are clearly visible at higher magnification (inset in Figure 3a and Figure S1 in the Supporting Information). Meanwhile, there are plenty of smoother regions which are "polymer-rich". These aggregates of nanorods are up to 100 nm in height. Because of these aggregations, the interfacial areas between polymer and CdSe are greatly reduced and this probably in turn reduced the amount of exciton dissociation at the interface. The aggregation in the film also resulted in incomplete transport pathways and hence a very low J_{SC}. Another film that shows substantial phase separation is the P3HT:CdSe-TEA film (Figure 3c). In this case, a substantial amount of DDPA was removed and this greatly affects the solubility of the nanorods in the solvent. This results in the aggregation of CdSe-TEA in the solution before they were blended into the polymer solution. In the CdSe-TMA case (Figure 3d), the removal of DDPA was less (γ_{DDPA} (TMA) = 0.17 compared to γ_{DDPA} (TEA) = 0.10, and the solubility of nanorods in solvent was better maintained and hence less phase separation occurred. As discussed earlier, the phase separated morphology in the CdSe-TEA film will probably result in poorer charge transport and hence the lower J_{SC}. On top of this, phase segregation will also result in a higher series resistance that adversely affects the FF. For optimum device performance, phase separation between polymer and nanoparticles should be controlled. The degree of phase separation is governed by particle−particle, particle−polymer, and particle−solvent interactions.

The film cast from CdSe-PY nanorods (Figure 3b) appears to have the smallest morphological features as compared to the others. In this case, 10 vol % of pyridine was added into the host solvent to help in the dispersion of the pyridine-coated nanorods in solution. As a result, the CdSe nanorods formed better

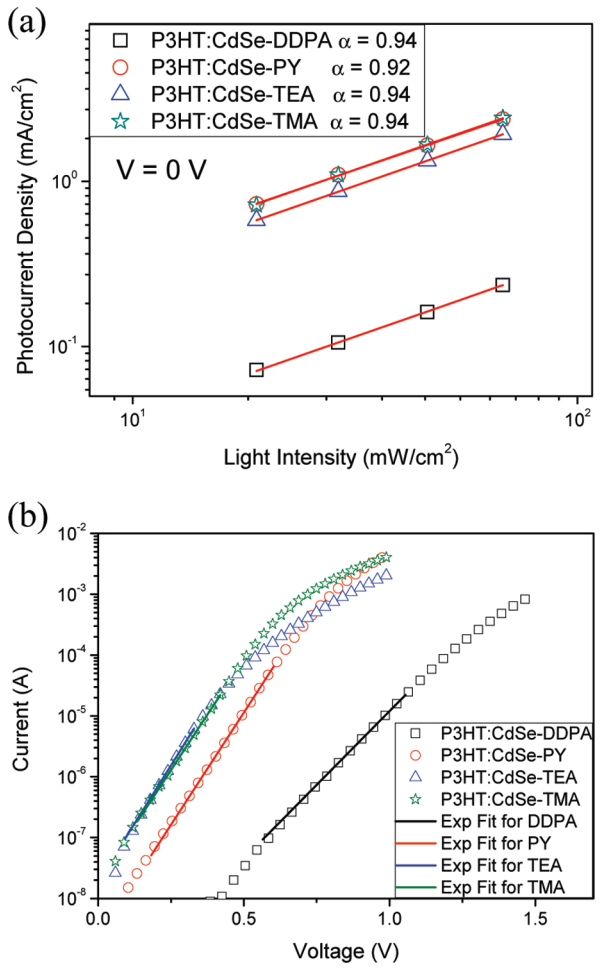

Figure 4. (a) Photocurrent density as a function of light intensity of four devices at the short circuit condition. Power law fits to $J_{ph} \propto I^{\alpha}$ are shown as solid lines. (b) Dark $I-V$ curve for P3HT:CdSe hybrid solar devices with different ligands with a semilog scale. Solid lines are fits to the exponential part with the Shockley formula for the 4 types of hybrid devices.

percolation pathways and hence enhanced the charge transport. This is reflected in the higher J_{SC} and FF. Better film morphology was also obtained for P3HT:CdSe-TMA films. This is favorable for charge transport and hence better device performance. Next, let us look at how these surface ligands affect the charge transport in such films.

The light intensity-dependent photocurrent was measured for all devices. Photocurrent densities of the devices as a function of light intensity were plotted at 0 V (Figure 4a). A power law $J_{ph} \propto I^{\alpha}$ (where I is the light intensity and J_{ph} is the photocurrent) was fitted to the data. CdSe-PY devices displayed an α value of 0.92, whereas for the other three devices, α is 0.94 at short circuit. Both α values are found to be less than 1, which can be due to two possible reasons. It can be caused by bimolecular recombination in devices with low mobilities, resulting in large charge densities.[19,20] It can also be caused by the space-charge effect in devices as a result of strong imbalance between electron and hole mobilities.[21] In this study, we observed a lower current density in the P3HT:CdSe-DDPA system compared to the other devices (Figure 4a), suggesting that the charge (electron) mobility in these devices is lower than in others, as the insulating DDPA shell prevents the polymers and nanorods coming closer to each other and hence hinders charge transfer. However, the α value for the DDPA system is similar other systems. This would suggest that in our systems, the space charge effect is responsible for the observed α. In highly imbalanced systems,α is rather insensitive to the recombination strength.

Semilog plots of the dark current−voltage ($I-V$) characteristic for all four devices are shown in Figure 4b. At lower applied bias voltage, current increases exponentially and the $I-V$ characteristic of these hybrid devices can be expressed by the Shockley equation: $I(V)=I_{sat}[e^{(qV/mkT)} - 1]$, where I_{sat} is the saturation current, q is the elementary charge constant, k the Boltzmann constant, m the ideality factor, and T is the absolute temperature.[19,22] At higher voltages, series resistance causes the current to increase slower, and the transition between the two regions is least clear in the device with DDPA. Fitting the exponential part of the curve with the Shockley formula gives ideality factors of 3.5 for DDPA and about 2.3 for the others. Such large values of m suggest that ligands form a potential barrier so the charge transport has to involve tunneling.[23] A lower m for the devices with exchanged ligands is consistent with the fact that these shorter molecules are more electron transparent than DDPA. When DDPA on the as-synthesized CdSe nanocrystals was partially replaced by new ligands, the currents were improved at least by 3 orders of magnitude. We therefore deduced that the distance between polymer and nanorods was reduced and most of the charge flowed through the replacing ligands.

CONCLUSIONS

In conclusion, we studied the effect of surface chemistry of CdSe nanorods on charge generation and charge transport in P3HT-CdSe hybrid solar cells based on the photovoltaic properties and intensity-dependent photocurrent. We have shown that the PCE of the hybrid devices increased at least 3-fold after ligand exchange with small molecules as a result of reduced distance between polymer/nanorods and nanorods/nanorods. The dark current for the ligand exchanged samples increased by 3 orders of magnitude compared to the pristine sample which implied that the resistance from the organic ligands is one of the current controlling factors. We also demonstrated that the combination of ligand exchange efficiency and dispersion are able to explain the variation in the device performances. Therefore, when selecting a surface ligand for nanoparticles, the size of the ligand, the conductivity, together with the ligand−solvent and ligand−polymer interaction, as well as the degree of ligand exchange have to be considered for the best hybrid solar cell device performance. Good device performance requires good charge transport between the nanoparticles and the polymer, and at the same time, the surface of the nanoparticles has to be compatible with the solvent and the polymer used. Rather than a single type of ligand on these surfaces, a combination of ligands may be a better option to obtain good hybrid films for solar cell device application.

ASSOCIATED CONTENT

Supporting Information. Summary of P3HT:CdSe hybrid device performance with different surface ligands using chloroform as the host solvent and AFM images of the P3HT:CdSe-DDPA blend film (PDF). This material is available free of charge via the Internet at http://pubs.acs.org/.

AUTHOR INFORMATION

Corresponding Author
*E-mail: ymlam@ntu.edu.sg.

ACKNOWLEDGMENT

We acknowledge technical assistance and contributions from Kwan Hang Lam, Ja Vui Chung, and Kheng Hwee Chua. This work was supported by Robert Bosch (SEA) Pte Ltd and the Science and Engineering Research Council, Agency for Science, Technology and Research (A*STAR), Singapore.

REFERENCES

(1) Li, G.; Shrotriya, V.; Huang, J.; Yao, Y.; Moriarty, T.; Emery, K.; Yang, Y. *Nat. Mater.* **2005**, *4*, 864–868.
(2) Ma, W.; Yang, C.; Gong, X.; Lee, K.; Heeger, A. J. *Adv. Funct. Mater.* **2005**, *15*, 1617–1622.
(3) Huynh, W. U.; Dittmer, J. J.; Libby, W. C.; Whiting, G. L.; Alivisatos, A. P. *Adv. Funct. Mater.* **2003**, *13*, 73–79.
(4) Sun, B.; Greenham, N. C. *Phys. Chem. Chem. Phys.* **2006**, *8*, 3557–3560.
(5) Sun, B.; Marx, E.; Greenham, N. C. *Nano Lett.* **2003**, *3*, 961–963.
(6) Huynh, W. U.; Dittmer, J. J.; Alivisatos, A. P. *Science* **2002**, *295*, 2425–2427.
(7) Saunders, B. R.; Turner, M. L. *Adv. Colloid Interface Sci.* **2008**, *138*, 1–23.
(8) Kumari, K.; Kumar, U.; Sharma, S. N.; Chand, S.; Kakkar, R.; Vankar, V. D.; Kumar, V. *J. Phys. D: Appl. Phys.* **2008**, *41*, 235409.
(9) Olson, J. D.; Gray, G. P.; Carter, S. A. *Sol. Energy Mater. Sol. Cells* **2009**, *93*, 519–523.
(10) Seo, J.; Kim, W. J.; Kim, S. J.; Lee, K.-S.; Cartwright, A. N.; Prasad, P. N. *Appl. Phys. Lett.* **2009**, *94*, 133302–3.
(11) Aldakov, D.; Chandezon, F.; Bettignies, R. D.; Firon, M.; Reiss, P.; Pron, A. *Eur. Phys. J. Appl. Phys.* **2006**, *36*, 261–265.
(12) Milliron, D. J.; Alivisatos, A. P.; Pitois, C.; Edder, C.; Fréchet, J. M. J. *Adv. Mater.* **2003**, *15*, 58–61.
(13) Xi, L.; Lam, Y. M. *Chem. Mater.* **2009**, *21*, 3710–3718.
(14) Murray, C. B.; Norris, D. J.; Bawendi, M. G. *J. Am. Chem. Soc.* **1993**, *115*, 8706–8715.
(15) Peng, Z. A.; Peng, X. *J. Am. Chem. Soc.* **2002**, *124*, 3343–3353.
(16) Foos, E. E.; Wilkinson, J.; Mäkinen, A. J.; Watkins, N. J.; Kafafi, Z. H.; Long, J. P. *Chem. Mater.* **2006**, *18*, 2886–2894.
(17) Kuno, M.; Lee, J. K.; Dabbousi, B. O.; Mikulec, F. V.; Bawendi, M. G. *J. Chem. Phys.* **1997**, *106*, 9869–9882.
(18) Yin, Y.; Alivisatos, A. P. *Nature* **2005**, *437*, 664–670.
(19) Huynh, W. U.; Dittmer, J. J.; Teclemariam, N.; Milliron, D. J.; Alivisatos, A. P.; Barnham, K. W. J. *Phys. Rev. B* **2003**, *67*, 115326.
(20) Yang, L.-G.; Chen, F.; Xu, H.; Wang, M.; Chen, H.-Z. *J. Appl. Phys.* **2009**, *106*, 073701–7.
(21) Koster, L. J. A.; Mihailetchi, V. D.; Xie, H.; Blom, P. W. M. *Appl. Phys. Lett.* **2005**, *87*, 203502–3.
(22) Sze, S. M. *Physics of Semiconductor Devices*; Wiley: New York, 1981.
(23) Yan, D.; Lu, H.; Chen, D.; Zhang, R.; Zheng, Y. *Appl. Phys. Lett.* **2010**, *96*, 083504–3.